iScience

CellPress
OPEN ACCESS

Article

Haploinsufficiency of the sex-determining genes at *MATα* restricts genome expansion in *Saccharomyces cerevisiae*

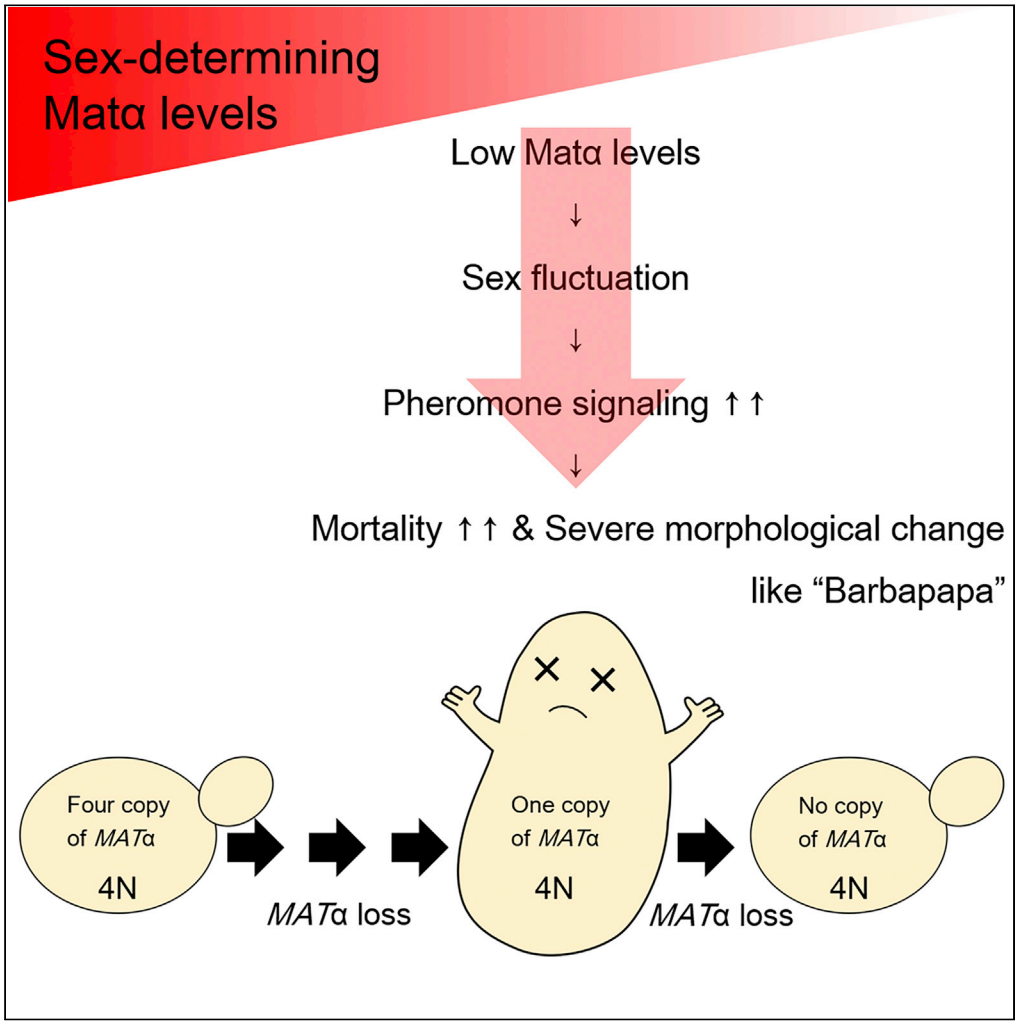

Kazumasa Oya,
Akira Matsuura

amatsuur@faculty.chiba-u.jp

Highlights

Polyploid cells with reduced *MATα* copies show abnormal morphology and increased death

These phenotypes are due to hyperactivation of the mating pheromone response pathway

Quantity of the *MATα* products is important for stable sexual phenotype

This property may be involved in the suppression of speciation via polyploidization

Oya & Matsuura, iScience *25*, 104783
August 19, 2022
https://doi.org/10.1016/j.isci.2022.104783

iScience

CellPress
OPEN ACCESS

Article

Haploinsufficiency of the sex-determining genes at *MATα* restricts genome expansion in *Saccharomyces cerevisiae*

Kazumasa Oya[1] and Akira Matsuura[2,3,*]

SUMMARY

In *Saccharomyces cerevisiae*, mating type of haploid cells is determined by the presence or absence of the *MATα* idiotype containing *MATα1* and *MATα2*, which encode the transcription factors. These proteins are characterized by rapid turnover, but the physiological relevance of this property remains unclear. Here, we show a direct link between their intracellular levels and sexual stability. Polyploid cells with fewer *MATα* copies had unstable sexual phenotypes, causing morphological changes and an increase in cell death; these effects were mediated by hyperactivation of the mating pheromone response pathway. Thus, the *MATα1* and *MATα2* genes are haploinsufficient genes, and the reduction in their product levels causes sex fluctuation. Chromosome III harboring the mating type locus is the most prone to loss in diploids. We propose that the haploinsufficiency of *MATα* compensates for the drop-out prone nature of chromosome III, thereby suppressing speciation through increased genome size via polyploidization.

INTRODUCTION

Because of its relevance to development, behavior, evolution, and diversity, the mechanism of sex determination has been studied extensively. Sexual dimorphism controlled by the sex-determination system is ubiquitous among eukaryotic organisms from yeasts to humans. Genetic analysis has allowed extensive analysis of the regulation of dichotomous sex and reproduction in the budding yeast *Saccharomyces cerevisiae* (Herskowitz, 1988). *S. cerevisiae* haploid cells show either an a- or α-mating type; mating two cells of different mating types produces an a/α diploid. Yeast mating types are determined by the mating type (*MAT*) locus, which is located on chromosome III and contains either the *MAT*a or *MATα* idiotype (Klar, 1987). Mata1, which is expressed from *MAT*a, and Matα1 and Matα2, which are expressed from *MATα*, are transcription factors with multiple targets that give rise to the differences among these three distinct cell types (Galgoczy et al., 2004). *MATα* contributes to determining haploid mating type, with Matα1 promoting expression of α-specific genes (*αsg*) and Matα2 suppressing a-specific genes (*asg*) (Strathern et al., 1981). In contrast, *MAT*a is involved in the repression of haploid-specific genes (*hsg*) in diploid cells but not in the determination of the haploid mating type (Strathern et al., 1981). Therefore, the sexual phenotype (a or α) in haploid yeast is determined by the presence or absence of the *MATα* (Hanson and Wolfe, 2017).

Because chromosome III is equivalent to sex chromosomes in other eukaryotes, the *MAT* locus and chromosome III may be involved in speciation, analogous to sex chromosomes in higher eukaryotes (Payseur et al., 2018). Chromosome III is among one of the shortest of 16 chromosomes in *S. cerevisiae*, and the most prone to loss in diploid yeast (Kumaran et al., 2013). Although an a/α diploid is intrinsically non-mating, it acquires mating ability upon loss of chromosome III, or when a *MAT* idiotype is mutated or deleted (Haber, 1974). In artificial hybridization by the rare mating of a diploid *S. cerevisiae* cell with a haploid *Saccharomyces kudriavzevii* spore/cell, the complete loss of one copy of chromosome III confers mating ability to *S. cerevisiae* (Morard et al., 2020). It has been speculated that the deletion of one idiotype at the *MAT* locus is also responsible for whole-genome duplication (WGD), as has occurred in the history of the Saccharomycetales lineage (Marcet-Houben and Gabaldón, 2015).

Previous studies have shown that the sex-determining *MATα* products show constant and rapid turnover during vegetative growth, so as not to interfere with mating type switching (Laney and Hochstrasser, 2003; Nixon et al., 2010). Therefore, we speculated that such *MATα* regulation is also involved in the

[1]Department of Biology, Graduate School of Science and Engineering, Chiba University, 1-33 Yayoi-chou, Inage-ku, Chiba 263-8522, Japan

[2]Department of Biology, Graduate School of Science, Chiba University, 1-33 Yayoi-chou, Inage-ku, Chiba 263-8522, Japan

[3]Lead contact

*Correspondence: amatsuur@faculty.chiba-u.jp

https://doi.org/10.1016/j.isci.2022.104783

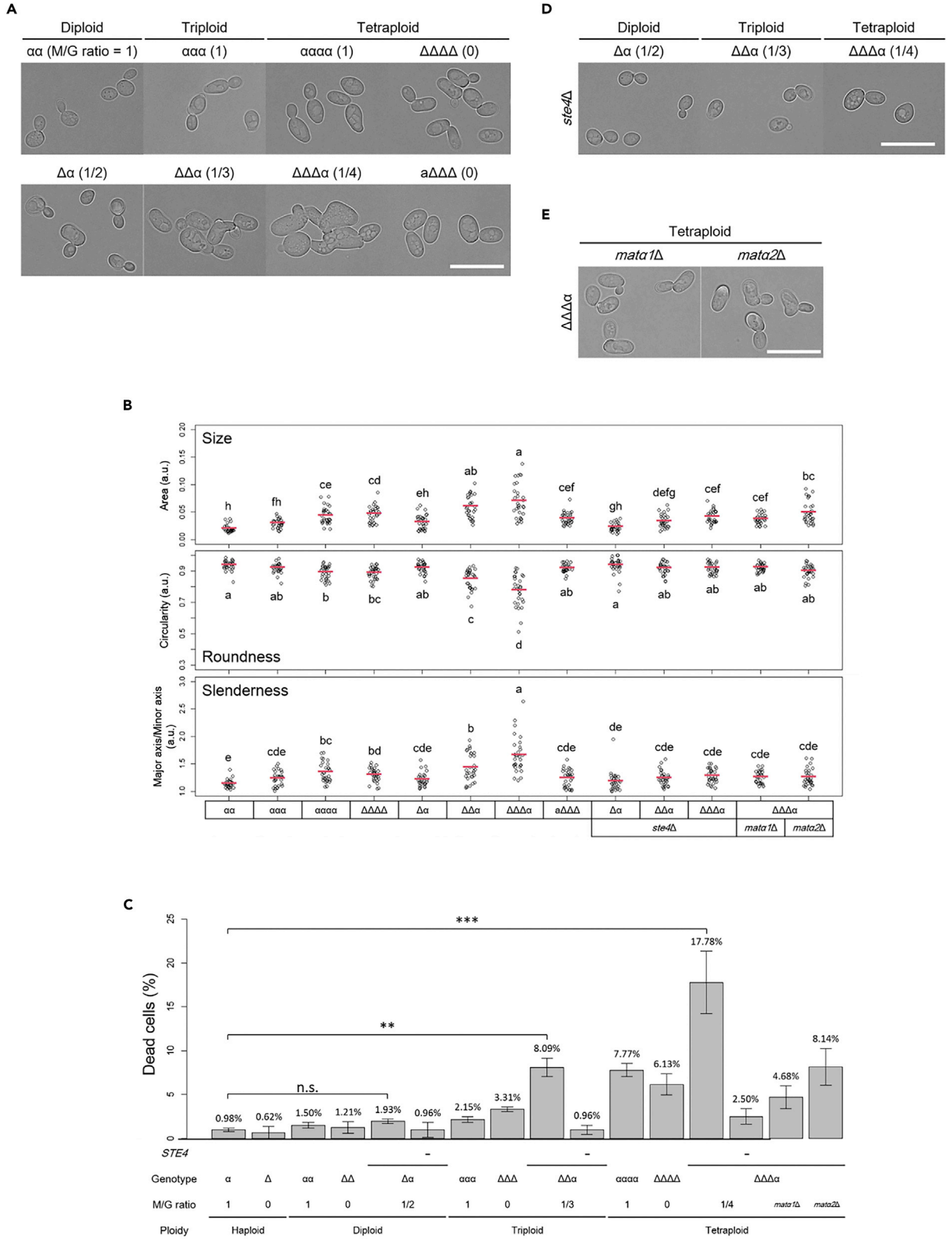
A
Diploid
Triploid
Tetraploid
αα (M/G ratio = 1)
ααα (1)
αααα (1)
ΔΔΔΔ (0)
Δα (1/2)
ΔΔα (1/3)
ΔΔΔα (1/4)
aΔΔΔ (0)
D
Diploid
Triploid
Tetraploid
Δα (1/2)
ΔΔα (1/3)
ΔΔΔα (1/4)
ste4Δ
E
Tetraploid
mata1Δ
mata2Δ
ΔΔΔα
B
Size
Area (a.u.)
Circularity (a.u.)
Roundness
Slenderness
Major axis/Minor axis (a.u.)
αα
ααα
αααα
ΔΔΔΔ
Δα
ΔΔα
ΔΔΔα
aΔΔΔ
Δα
ΔΔα
ΔΔΔα
ΔΔΔα
ste4Δ
mata1Δ
mata2Δ
C
Dead cells (%)
***
**
n.s.
0.98%
0.62%
1.50%
1.21%
1.93%
0.96%
2.15%
3.31%
8.09%
0.96%
7.77%
6.13%
17.78%
2.50%
4.68%
8.14%
STE4
Genotype
M/G ratio
Ploidy
Haploid
Diploid
Triploid
Tetraploid

Figure 1. A decrease in the M/G ratio affects cell morphology and mortality

(A) Microscopic observation to assess the effect of the M/G ratio on cell morphology. Scale bar = 20 μm.

(B) Bee swarm plots show the quantitative results of the images shown in Figures 1A, 1D, and 1E. Red bars represent mean values. The calculation of each parameter is described in Quantification and statistical analysis. Different letters represent significant differences, determined by one-way ANOVA and Tukey's HSD comparisons.

(C) Fractions of dead cells. The numbers above the graphs are mean values and the error bars indicate the SD(n = 3 experiments). To calculate the p value for M/G ratio mutants with one copy of *MATα* relative to WT *MATα* haploid, we applied the Dunnett's test; ***$p < 0.001$, **$p < 0.01$.

(D) Effect of *matα1*Δ and *matα2*Δ on the ΔΔΔα cell morphology. Scale bar = 20 μm.

(E) Effect of *ste4*Δ on the cell morphology of M/G ratio mutants. Scale bar = 20 μm.

expression of the sexual phenotype. In this study, we devised a method of controlling the levels of intracellular sex-determining transcription factors using polyploid yeast cells and addressed the relationship between their intracellular levels and sexual stability.

RESULTS

The copy number of sex-determining *MATα* genes affects polyploid cell morphology and death rate

To examine the effects of decreased levels of Matα proteins on the sexual phenotype in polyploid cells, we generated a series of mutants with altered ratios of the *MATα* copy number to genome set number (M/G ratio). We then examined the effect of the M/G ratio on mortality and morphological parameters such as size, roundness, and slenderness. In *MATα* polyploid strains with a normal M/G ratio of 1, cell size tended to increase, and cell shape tended to elongate, with increasing ploidy (αα, ααα, and αααα; Figure 1A). The ααα and αααα strains were significantly larger and longer (increased by 1.47 and 2.17 times in size and 1.08 and 1.18 times in slenderness, respectively) than the αα strain (Figure 1B), consistent with the findings of previous polyploidy studies (Galitski et al., 1999). Interestingly, we found that a decrease in the M/G ratio in *MATα* polyploid cells caused highly elongated, amorphous Barbapapa-like cell morphologies (ΔΔΔα; Figure 1A), which is typical of cells under prolonged exposure to mating pheromones or those that display activation of the abnormal/unsuppressed mating pheromone response pathway (mating pathway) (Siekhaus and Drubin, 2003; Tanaka and Yi, 2009; Udden and Finkelstein, 1978). The ΔΔΔα cells showed reduced circularity (0.89–0.77) and were 1.61 times larger and 1.23 times longer than αααα (Figure 1B). Diseased cells were apparent in the ΔΔΔα culture, as confirmed by selective propidium iodide (PI) staining of dead cells. The PI-positive fraction increased with ploidy, and as the M/G ratio decreased, the latter effect was independent of the ploidy level (Figure 1C). In comparison, tetraploid cells with complete loss of *MATα* (ΔΔΔΔ) and only one copy of *MATa* (aΔΔΔ; 6.13 ± 2.88%) had a lower percentage of dead cells compared to ΔΔΔα cells (Figures 1A and 1C). These cells were not significantly different from αααα cells in the morphological parameters (Figures 1A and 1B). These results are consistent with the observation that *mat*Δ cells with no *MATα* behave as an a-mating type (Strathern et al., 1981).

Since a high concentration of mating pheromones can induce rapid cell death (Zhang et al., 2006), we examined the relationship between the mating pathway and mortality in M/G ratio mutants. *STE4* encodes the beta-subunit of a heterotrimeric G protein downstream of mating pheromone receptors involved in the mating pathway; receptor signaling is blocked by the loss of Ste4 protein (Hartwell, 1980). In mutants lacking *STE4*, the morphological changes induced by a reduced M/G ratio were suppressed regardless of ploidy; *ste4*Δ M/G ratio mutant strains were comparable to the ploidy-matched *MATα* polyploid strains in the three parameters (Figures 1B and 1D), and showed a decreased proportion of PI-positive cells (Figure 1C), indicating that the phenotypes induced by the decreased M/G ratio are dependent on the mating pathway. This result suggests that the ΔΔΔα Barbapapa-like morphology is caused by the activation of the mating pathway (Figure 1A).

Because Matα1 promotes *MATα*-specific gene expression, whereas Matα2 represses *MATa*-specific gene expression, we expected that *matα1*Δ ΔΔΔα and *matα2*Δ ΔΔΔα would show phenotypes similar to ΔΔΔΔ and ΔΔΔα, respectively. Unexpectedly, however, the abnormal morphologies were suppressed in the single mutants (Figures 1B and 1E). In particular, the induction of *matα1*Δ or *matα2*Δ resulted in the recovery of circularity (0.77 in ΔΔΔα to 0.92 or 0.90, respectively), which was close to the ΔΔΔΔ circularity (0.89). The increased cell death was also suppressed completely by *matα1*Δ and partially by *matα2*Δ (Figure 1C). These results indicate that the reduced expression of these two genes is involved in the synthesis of the ΔΔΔα phenotype.

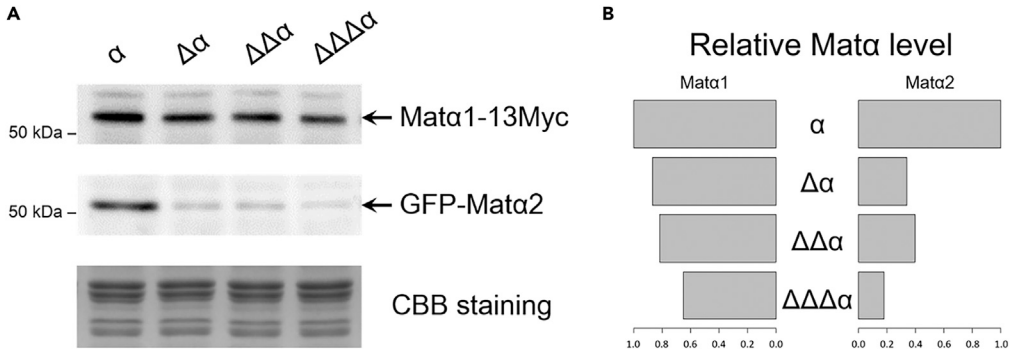

Figure 2. A decrease in the M/G ratio causes a decrease in the intracellular amounts of Matα1 and Matα2 proteins

(A) Western blot analysis of Matα1-13Myc and GFP-Matα2. Coomassie Brilliant Blue (CBB) staining corresponding to the Western blot is shown in the bottom panel. The total protein content of the samples was adjusted by CBB staining prior to the SDS-PAGE. With these samples, detection by anti-Myc and anti-GFP is performed in independent membranes.

(B) Bar graphs show the relative ratio of Matα1 and Matα2 corrected by CBB staining.

We then quantified the amounts of Matα1 and Matα2 proteins in M/G ratio mutants by Western blotting. Both proteins decreased with the M/G ratio, with Matα2 exhibiting greater depletion (Figures 2A, 2B, and S1). Previous studies estimated the half-lives of Matα1 and Matα2 as ~15 and ~5 min, respectively (Hochstrasser and Varshavsky, 1990; Nixon et al., 2010). Therefore, we speculated that the different effects of the M/G ratio on the amounts of Matα1 and Matα2 were due to the differences in their respective half-lives.

Finally, we examined the effect of the M/G ratio using a series of ectopic *MATα* expressed from loci other than the native *MAT*. Aberrant morphologies were observed at an M/G ratio of <1, with a lower M/G ratio associated with greater severity of aberrant morphology; the introduction of ectopic *MATα* reversed the abnormal morphology of M/G ratio mutants (Figure 3A). For each ploidy, a decrease in roundness and an increase in size and slenderness were observed when the M/G ratio was less than 1 (Figure 3B). Complementation with ectopic *MATα* also normalized mortality to the same rate as in the wild type (*MATα* + 3 × ectopic *MATα* tetraploid; 4.92 ± 2.99%). These results confirmed that the phenotype of M/G ratio mutants was dependent on the relative copy number of *MATα*, and indicated that reduced expression of the sex-determining *MATα* has adverse effects on *S. cerevisiae* cells.

Cells with a decreased M/G ratio cannot maintain a stable sexual phenotype

As described above, the morphology of M/G ratio mutants is associated with the mating pathway. Activation of the mating pathway requires the presence of both mating type cells, or at least the simultaneous expression of a pheromone specific to one mating type cell and its receptor normally expressed in cells of the other mating type. Since the phenotypes of the M/G ratio mutants suggest an abnormality in the sex-determination system, we generated fluorescent reporters that facilitated monitoring the expression of mating type-specific genes. These reporters express green fluorescent protein (GFP) and mCherry downstream of the promoters of *MAT*a-specific *MFA1* and *MATα*-specific *MFALPHA1*, respectively, which enables mating type discrimination by fluorescence observation. As expected, GFP fluorescence was observed in wild-type (WT) *MAT*a cells, mCherry fluorescence was observed in WT *MATα* cells, and no fluorescence was observed in WT *MAT*a/*MATα* diploid cells (Figure 4A). Moreover, no fluorescence was observed in haploid *matα1*Δ cells that lost the expression of both a*sg* and α*sg* (Bender and Sprague, 1989), and fluorescence of both was observed in *matα2*Δ cells (which express both a*sg* and α*sg*) (Bender and Sprague, 1989), confirming the efficacy of our fluorescence mating type reporters (Figure 4A). We found that ΔΔΔα emitted not only red fluorescence but also some green fluorescence, although it is genetically *MATα* (Figure 4A). This suggests that the M/G ratio mutants cannot stably express either the a- or α-mating type, leading to sex fluctuation.

Our observations with the mating type reporters suggested that not only the pheromone-encoding genes used to make the reporters but also other a- and α-specific genes, such as receptors, were expressed abnormally. We noticed that the mCherry fluorescence of ΔΔΔα cells was markedly higher than that of α cells (Figure 4B), suggesting that the activity of the *MFALPHA1* promoter is enhanced in ΔΔΔα cells. As the expression of mating pheromone genes was activated by the mating pathway (Roberts et al., 2000;

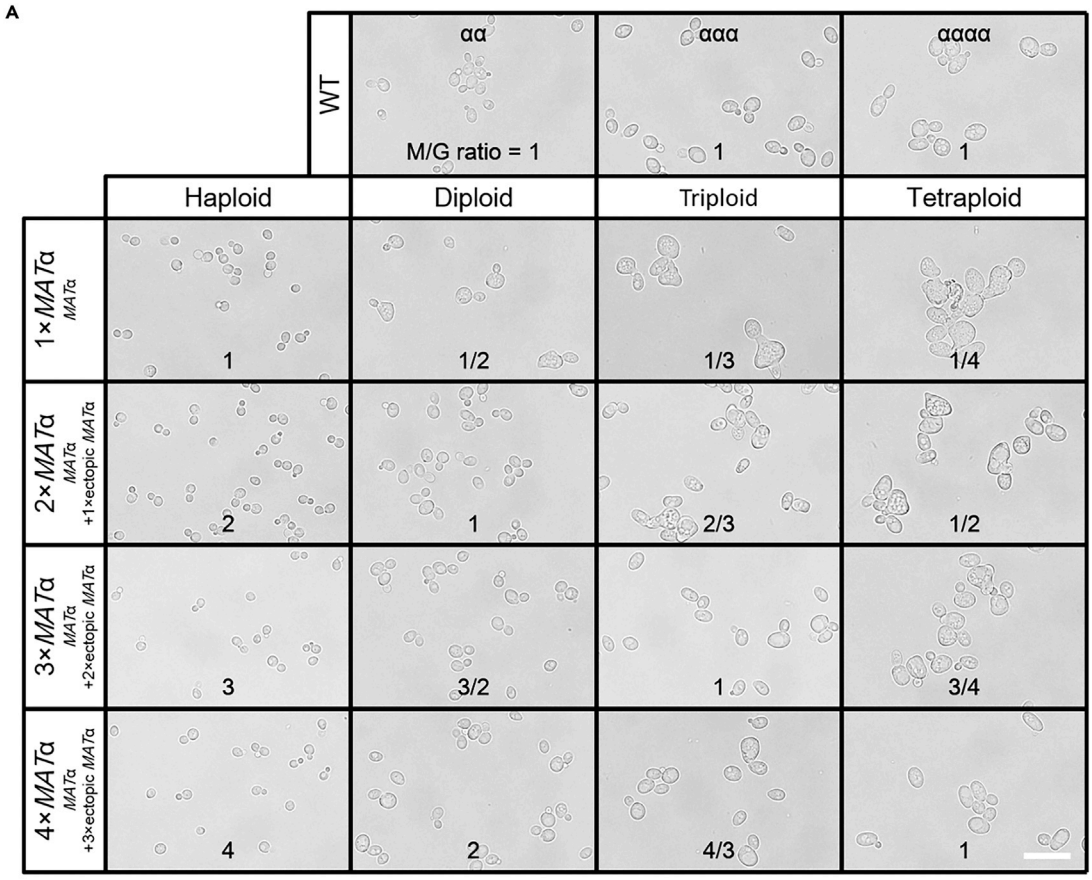
A
WT
αα
M/G ratio = 1
ααα
1
αααα
1
Haploid
Diploid
Triploid
Tetraploid
1×MATα
MATα
1
1/2
1/3
1/4
2×MATα
MATα
+1×ectopic MATα
2
1
2/3
1/2
3×MATα
MATα
+2×ectopic MATα
3
3/2
1
3/4
4×MATα
MATα
+3×ectopic MATα
4
2
4/3
1

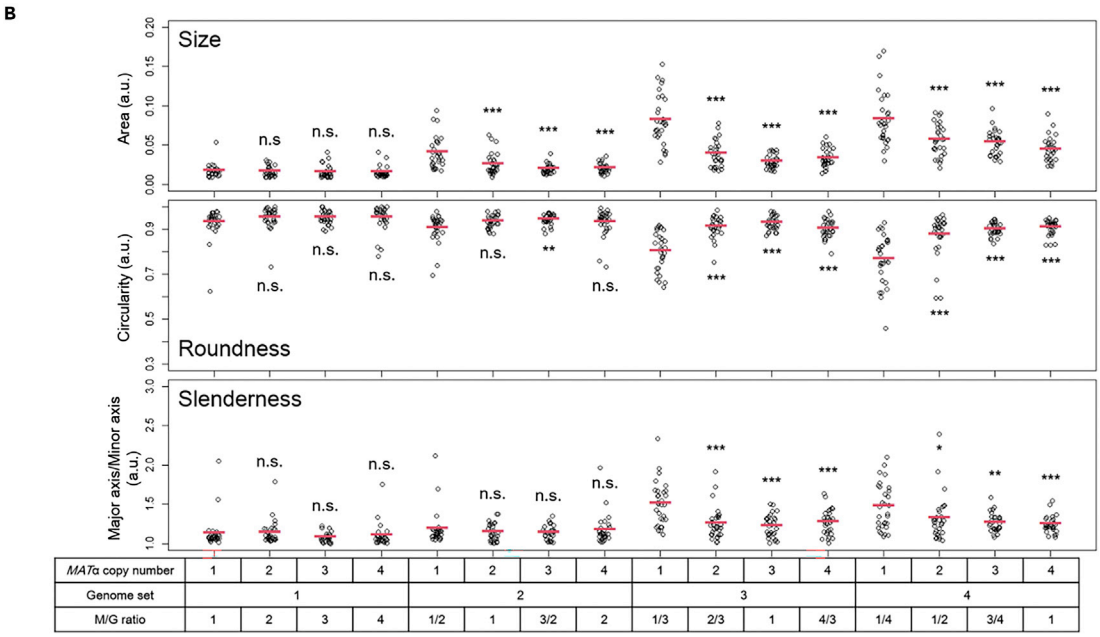
B
Size
Area (a.u.)
Circularity (a.u.)
Roundness
Slenderness
Major axis/Minor axis (a.u.)
MATα copy number
Genome set
M/G ratio

Figure 3. Ectopic *MATα* expression suppresses the phenotypes of M/G ratio mutants

(A) Bright-field images for analyzing M/G ratio values according to cell morphology. Scale bar = 20 μm. The numbers in the figure are the M/G ratios for each strain.

(B) Bee swarm plots show the quantitative results of the images shown in Figure 3A. Red bars represent mean values. The calculation of each parameter is described in Quantification and statistical analysis. The p value was calculated by the Dunnett's test using strains with one copy of *MATα* in each ploidy as a control group; ***$p < 0.001$, **$p < 0.01$, *$p < 0.05$.

Strazdis and MacKay, 1983), we suspected that, in M/G ratio mutants, pheromones secreted by mutants or their clones bind to their "own" receptors, thereby activating the mating pathway even in clones derived from a single cell.

The mating pathway is hyperactivated in cells with a lower M/G ratio

Since mating type instability is thought to activate the mating pathway via the binding of mating pheromones to their receptors, we verified the fluorescence intensity of *FUS1pr*-GFP, using flow cytometry to evaluate the activation level of the mating pathway in the M/G ratio mutants. The *FUS1* promoter is commonly used to measure the transcriptional response of the mating pathway (Banderas et al., 2016; Hagen et al., 1991; Paliwal et al., 2007; Takahashi and Pryciak, 2008). Indeed, the M/G ratio mutants had greater *FUS1pr*-GFP fluorescence, indicating mating pathway activation (Figure 4C). However, the activity of our *FUS1pr*-GFP reporter was saturated in mutants with M/G ratios of 1/3 and 1/4. The reporter activity in these mutants was much higher than that of the *matα2*Δ and *sst2*Δ mutants, which are constitutively activated mating pathway mutants (Figure 4C) (Bender and Sprague, 1989; Siekhaus and Drubin, 2003). Thus, hyperactivation of the mating pathway explains the high death rate (Figure 1C) in M/G ratio mutants.

Morphological changes and a high percentage of dead cells in the M/G ratio mutants are not observed after mating with *MAT*a cells

Consistent with the mating type instability phenotype (Figures 4A–4C), M/G ratio mutants showed substantial mating with *MATα* cells, in addition to normal mating with *MAT*a cells (Figure 5A). However, no octaploid cells formed when ΔΔΔα was cultured alone, under conditions where triploid cells formed by mating in a co-culture of haploid *mat*Δ cells and haploid *MATα* cells (Figure S2), suggesting that the phenotype of M/G ratio mutants mating with *MATα* cells is unstable. This indicates that the bimater phenotype of M/G ratio mutants is caused by mating type fluctuation, and not solely by chromosome loss, which was reported to occur in polyploid mitosis (Comai, 2005; Kumaran et al., 2013; Mayer and Aguilera, 1990).

Interestingly, M/G ratio mutants showed no morphological changes; despite the increase in ploidy, the ΔΔα and ΔΔΔα strains were smaller and shorter (reduced by 0.81 and 0.75 times in size and 0.93 and 0.79 times in slenderness, respectively) after mating with *MAT*a cells (Figures 5B and S3). Moreover, mating with *MAT*a cells resulted in fewer PI-positive in ΔΔΔα cells (tetraploid ΔΔΔα; 17.78 ± 2.92% to pentaploid aΔΔΔα; 10.81 ± 3.71%). The Mata1, Matα1, and Matα2 transcription regulators, which are involved in controlling the expression of mating type-specific genes, are rapidly turned over by degradation of control of the ubiquitin proteasome system (Johnson et al., 1998; Laney and Hochstrasser, 2003; Nixon et al., 2010). By contrast, in the a/α diploid with both *MAT*a and *MATα* idiotypes formed by mating, Mata1 and Matα2 are stabilized by binding to each other and forming an a1-α2 repressor (Johnson et al., 1998). This supports our model, in which the phenotypes of M/G ratio mutants are due to rapid turnover of Matα proteins normally found in *MATα* haploid cells, and shows that the expression of Matα proteins with a reduced number of *MATα* copies is sufficient for function if the product is stabilized after mating.

DISCUSSION

The *S. cerevisiae* mating type determination system harbors instability

Although it was previously thought that the *S. cerevisiae* mating type was determined by the presence or absence of *MATα* (Hanson and Wolfe, 2017), we show that the amount of *MATα* products is also important for sex determination; furthermore, we found that an insufficient quantity of *MATα* products induces unstable sex-specific gene expression (Figures 4A and 4B). We speculate that this is due to the rapid turnover of *MATα* products. In addition to the regulation of Matα proteins turnover described above, it is interesting to note that the expression of *MATα1* is repressed in the presence of the a1-α2 repressor (Johnson, 1995). In fact, we observed that, in the a/α-mating type state, a decrease in *MATα* products was not problematic (Figures 5B and S3), which supports the idea that this phenomenon is caused by rapid turnover. Nixon et al. (2010) discussed that the rapid turnover prevents simultaneous display of both a- and α-mating

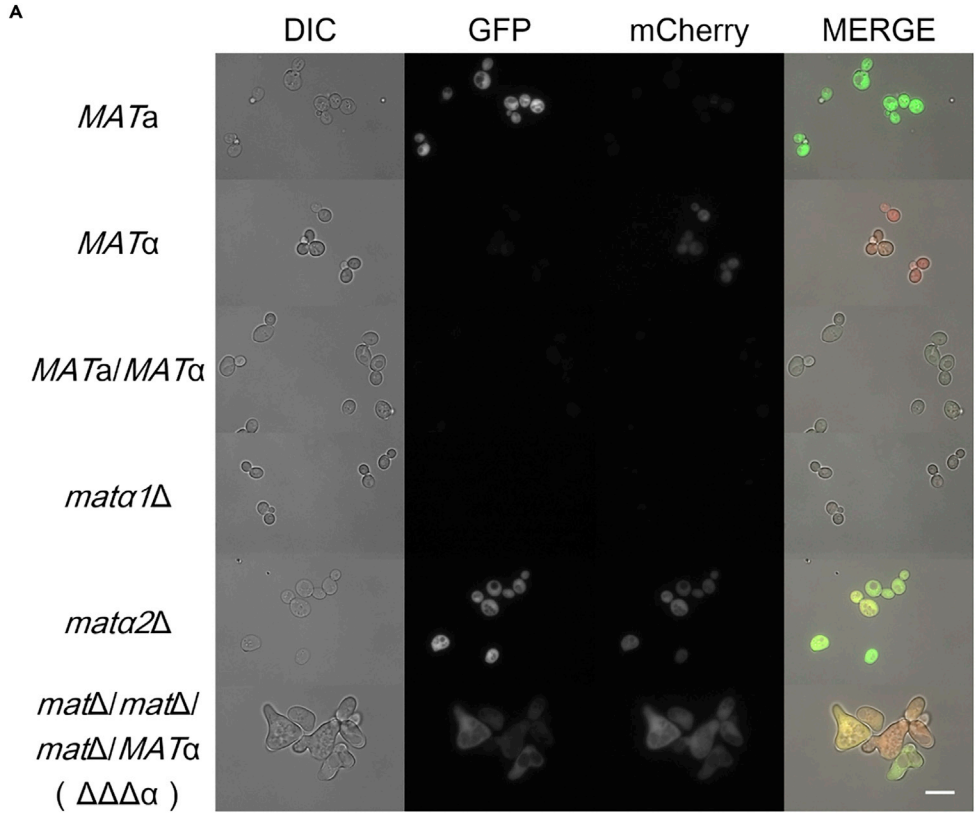
A
DIC
GFP
mCherry
MERGE
MATa
MATα
MATa/MATα
matα1Δ
matα2Δ
matΔ/matΔ/
matΔ/MATα
(ΔΔΔα)

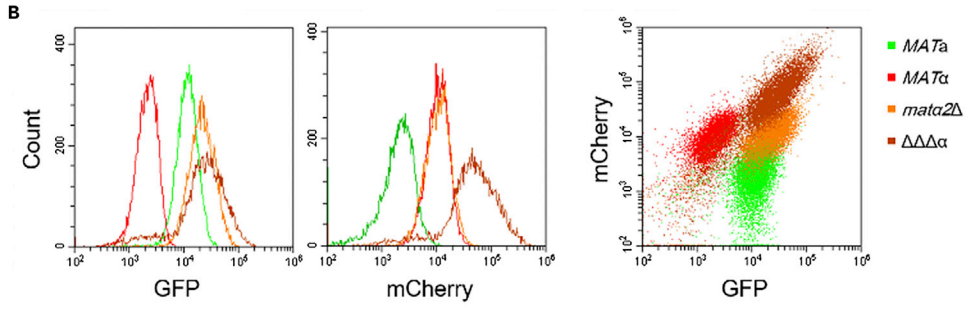
B
Count
GFP
mCherry
MATa
MATα
matα2Δ
ΔΔΔα

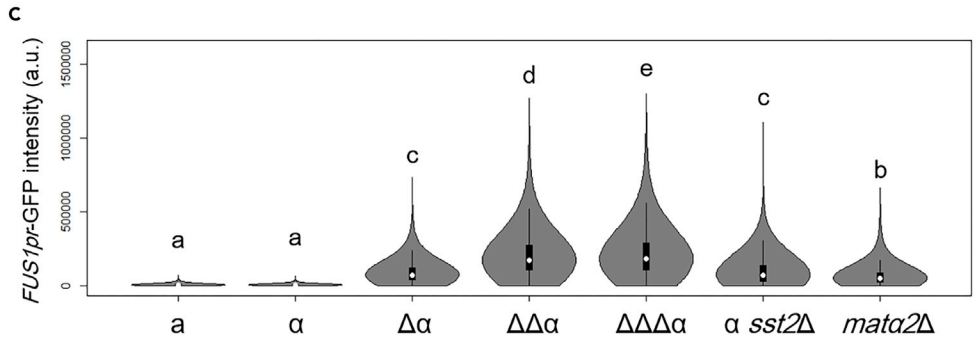
C
FUS1pr-GFP intensity (a.u.)
a
a
c
d
e
c
b
a
α
Δα
ΔΔα
ΔΔΔα
α sst2Δ
matα2Δ

Figure 4. M/G ratio mutants are unable to maintain a stable sexual phenotype

(A and B) Fluorescence of the mating type reporters, *MFA1pr*-GFP and *MFALPHA1pr*-mCherry acquired by fluorescence microscopy (A) and flow cytometry (B) show the sexual phenotype and its intensity. Scale bar = 10 μm. Histograms and plots show each fluorescence intensity and its variation (n = 10,000).

(C) Violin plots show the activation level of the mating pathway, determined by measuring the fluorescence of *FUS1pr*-GFP with flow cytometry (n = 10,000). Letters represent significant differences, determined by one-way ANOVA and Tukey's HSD comparisons.

type phenotypes during mating type switching, and does not interfere with the definition of the new mating type (Nixon et al., 2010). Consistently, pheromone receptors, which are the most upstream factors in the mating pathway, are constitutively taken up by endocytosis (Davis et al., 1993; Jenness and Spatrick, 1986).

In this study, we demonstrated the impact of decreased *MAT*α products on sexual identity and mating using polyploid cells. We previously observed Barbapapa-like cells when Matα proteins were expressed from *MAT*α on a centromeric plasmid in haploid *mat*Δ cells (unpublished observation). Since plasmid-borne gene expression is highly variable from cell to cell (Chou et al., 2015), we assume that this phenotype is caused by a shortage of Matα proteins in a fraction of cells with low expression of *MAT*α genes from the plasmid. Thus, we speculate that the ratio of *MAT*α-derived protein amounts to genome size is critical for the stable expression of the sexual phenotype regulated by *MAT*α, irrespective of the ploidy.

Low levels of Matα proteins result in mating pathway confusion

In homothallic strains of *S. cerevisiae*, switching between the a- and α-mating type phenotypes is completed within the span of a single division cycle, and pheromones and receptors, for example, must also be replaced within this span (Herskowitz, 1988). The mating type reporters used in this study were based on free GFP and mCherry, and their half-lives in yeast cells are longer than the duration of the cell cycle (Mateus and Avery, 2000; Natarajan et al., 1998). This property allows the respective fluorescence emission to continue even after the corresponding gene is repressed. Therefore, our reporters represent sexual history rather than the sex at the moment. Taking advantage of this character, we demonstrated that a decrease in *MAT*α copy number in polyploid cells caused sex fluctuation, as manifested by the expression of a*sg* and α*sg* (Figures 4A and 4B), and hyperactivation of the mating pathway (Figure 4B). In addition, hyperactivation was also manifested by strong expression of *FUS1pr*-GFP (Figure 4C).

Although ΔΔΔα cells exhibited abnormal a*sg* gene expression, they still behaved as the α-mating type, as judged by rare mating with an α-mating type tester (Figure 5A) and no conspicuous mating in ΔΔΔα culture (Figure S2). Our reporters, which reflect the expression of mating pheromones, provide insight into the specific phenotype of ΔΔΔα and the underlying mechanisms by revealing the sexual history. ΔΔΔα showed a bias toward mCherry over GFP, i.e., stronger expression of α*sg* than a*sg* (Figure 4B). Furthermore, our reporter analysis revealed intriguing differences in the expression levels of α*sg* and a*sg* between *matα2*Δ and ΔΔΔα, although the expression of a*sg* was derepressed in both mutants (Figures 4A–4C).

When a and α cells are fused to form a zygote, activity of the mating pathway is attenuated through the interaction of *MAT*a-specific Asg7 and *MAT*α-specific Ste3 (Roth et al., 2000). Our flow cytometry data showed that the expression levels of GFP and mCherry in *matα2*Δ were comparable to those in *MAT*a and *MAT*α, respectively (Figure 4B), despite activation of the mating pathway (Figure 4C). This was presumably mediated by the attenuation of the mating pathway through the interaction of *MAT*a-specific Asg7 and *MAT*α-specific Ste3, which is thought to be important in the zygotic fusion event (Roth et al., 2000) and was proposed to occur in *matα2*Δ cells (Rivers and Sprague, 2003). By contrast, ΔΔΔα expressed less a*sg* than α*sg*, which would result in insufficient attenuation by Asg7-Ste3, causing hyperactivation of the mating pathway. In conclusion, we assume that ΔΔΔα, which is genetically *MAT*α, causes pheromone-receptor-mediated activation of the mating pathway due to transient expression of the a-mating type phenotype caused by a quantitative deficiency of *MAT*α products.

*MAT*α is composed of haploinsufficient genes encoding transcription factors

The above-described properties are related to the fact that the two proteins expressed from *MAT*α, Matα1 and Matα2, are transcription factors with multiple targets. In cells expressing *MAT*α, Matα1 promotes α*sg* expression and Matα2 represses a*sg* expression, so that the cells stably express the α-mating type (Strathern et al., 1981). It is conceivable that, if the amount of each *MAT*α product is insufficient, the transcriptional

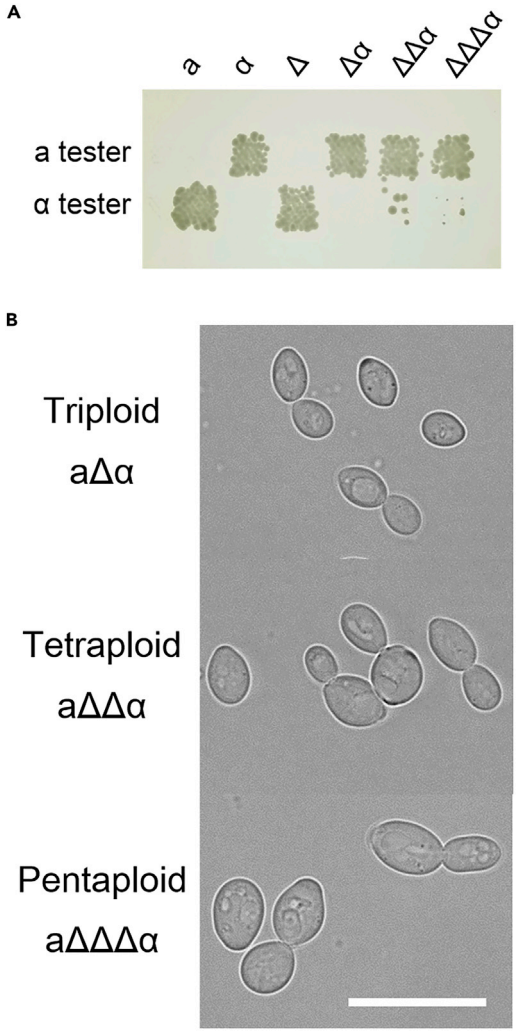

Figure 5. M/G ratio mutants still maintain the α-mating type, and their phenotypes are normalized after mating

(A) Confirmation of mating type through mating with a- and α-tester strains. As selection markers, tester strains have the *LEU2* gene and sample strains have the *HIS3* gene. On the SC -Leu -His plate, only zygotes could grow.

(B) Effect of mating with a *MAT*a cell on the cell morphology of M/G ratio mutants. Scale bar = 20 μm.

state of all target genes cannot be maintained. In other words, *MAT*α products have a threshold for the sexual phenotype, and the morphological changes and increased mortality in M/G ratio mutants occurred (Figures 1A–1C, 3A, and 3B) because it was below this threshold (Figures 2A and 2B).

For Matα2 to act as a transcriptional repressor, it needs to form a complex with Mcm1, which is also involved in cell cycle regulation (Herskowitz, 1989; Keleher et al., 1988). Apart from the prediction that the overproduction of *MAT*α products interferes with mating type switching (Laney and Hochstrasser, 2003; Nixon et al., 2010), we confirmed that *MAT*α*2* overexpression causes phenotypes such as growth defects (Figure S4). Since loss-of-function *MCM1* mutants have a similar phenotype (Lim et al., 2003), this result may be due to the depletion of Mcm1 by preferential complex formation by excessive Matα2. Taken together with our finding that the phenotype of a *MAT*α polyploid depends on the amount of intracellular Matα (Figures 1A–1C, 2A, 2B, 3A, 3B, and 4A–4C), these data argue for the need to balance the expression of *MAT*α, neither too much nor too little. This is in line with the dosage-stabilizing hypothesis explaining haploinsufficient (HI) genes, such that a decrease in expression of their products causes a decrease in fitness, while an increase in expression is toxic (Morrill and Amon, 2019). We speculate that *MAT*α has evolved as an HI idiotype.

HI genes are thought to be "stuck" in evolutionary terms, i.e., are unable to regulate gene expression in response to gene dosage variation (Morrill and Amon, 2019). The narrow range of expression of HI genes and significantly reduced fitness when they are outside this range indicate that HI genes are highly sensitive to changes in genome size. The accumulation of HI genes on chromosome III is thought to be the result of selection pressure that prevents diploids from losing this chromosome (de Clare et al., 2011; Delneri et al., 2008). We hypothesize that the haploinsufficiency of *MATα*, which we discovered, also reduces the fitness of diploids with loss of function of *MATα* or loss of chromosome III. The loss of a *MATα* locus in diploids would lead to the production of triploid cells incapable of normal meiosis; *S. cerevisiae* must have evolved such a mechanism to suppress the emergence of such diploids. In other words, we speculate that the haploinsufficiency of the sex-determining transcription factor genes at *MATα* prevents diploids from re-entering the mating stage.

The haploinsufficiency in *MATα* idiotype suppresses genome expansion

Significant events in the genome evolution of *S. cerevisiae* include WGD and alterations to the sex-determination mechanism (Dujon and Louis, 2017; Hanson and Wolfe, 2017). WGD provides the potential for new functional divergence between paralogous genes and creates a reproductive barrier to ancestral species, leading to speciation (Otto, 2007). WGD is involved in speciation of *S. cerevisiae*, as indicated by genome comparison between *S. cerevisiae* and *Lachancea waltii* (Kellis et al., 2004). As for the mechanism of mating type determination, the transcriptional circuit regulating *asg* expression of the ancestral species was altered in *S. cerevisiae* (Hanson and Wolfe, 2017). Mata2, which activates *asg* expression in ancestral yeast a-mating type cells, was lost in the *S. cerevisiae* lineage, and *S. cerevisiae* now uses a Matα2 repressing mechanism of *asg* expression (i.e., expression *asg* by default) (Sorrells et al., 2015; Tsong et al., 2003). We speculate that *MATα* haploinsufficiency evolved after the loss of *MATa2* because it depends on the mating type determination mechanism that exhibits an a-mating type by default. It should be noted that the evolution of the *asg* regulatory circuit is assumed to occur at the same time as WGD, about 100 million years ago (Tsong et al., 2006; Wolfe and Shields, 1997).

Despite experiencing WGD, the current genome of *S. cerevisiae* is comparable in size to the genome of the pre-WGD yeast *L. waltii* (approximately 12 and 11 Mb, respectively) (Goffeau et al., 1996; Kellis et al., 2004). This suggests a size-limiting mechanism in the genome of *S. cerevisiae*, which may be the haploinsufficiency of *MATα* identified in this study. In conclusion, we speculate that the haploinsufficiency of *MATα* cooperates with HI genes accumulation on chromosome III to compensate for the loss-prone nature of chromosome III and to suppress speciation with an increased genome size.

Limitations of the study

This study demonstrated that the *MATα* idiotype is composed of HI genes and that the concentration of their products is involved in the stability of mating type in *S. cerevisiae*, suggesting that the haploinsufficiency of *MATα* may affect genome evolution of *S. cerevisiae*. Although spontaneous diploidization is a relatively common phenomenon under certain stressful conditions and polyploid cells can be easily produced (Galitski et al., 1999; Harari et al., 2018), WGD occurred only once, about 100 million years ago, in the Saccharomycetales lineage (Wolfe and Shields, 1997). We hypothesize that the accumulation of HI genes on the mating type chromosome and the haploinsufficiency of *MATα* may explain why WGD was an unusual event in the history of the order Saccharomycetales. However, since our research has so far focused exclusively on *S. cerevisiae*, we have not been able to discuss the evolution of Saccharomycetales. It would be interesting to address the haploinsufficiency of sex-determining genes in species other than *S. cerevisiae* in a future study.

STAR★METHODS

Detailed methods are provided in the online version of this paper and include the following:

- KEY RESOURCES TABLE
- RESOURCE AVAILABILITY
  - Lead contact
  - Materials availability
  - Data and code availability
- EXPERIMENTAL MODEL AND SUBJECT DETAILS
- METHOD DETAILS
  - Yeast strains, plasmids, and media

- Microscopy
- Analysis of mating type reporters
- Analysis of *FUS1pr*-GFP reporter
- Quantification of live/dead cells
- Mating test
- Western blot analysis
- DNA content measurement
- Spot assay

- QUANTIFICATION AND STATISTICAL ANALYSIS
  - Microscopy image analysis

SUPPLEMENTAL INFORMATION

Supplemental information can be found online at https://doi.org/10.1016/j.isci.2022.104783.

ACKNOWLEDGMENTS

We thank Drs. Koei Okazaki, Takashi Tsuchimatsu, and Eigo Takeda, and members of Matsuura laboratory for valuable discussions, and Textcheck for editing the manuscript. We also thank anonymous reviewers for critically reading the manuscript and suggesting substantial improvements. This work was supported by JST SPRING, Grant Number JPMJSP2109.

AUTHOR CONTRIBUTIONS

Conceptualization, K.O. and A.M.; Methodology, K.O. and A.M.; Investigation, K.O.; Resources, K.O. and A.M.; Writing - Original Draft, K.O.; Writing - Review and editing, A.M.; Funding Acquisition, K.O. and A.M.

DECLARATION OF INTERESTS

The authors declare no competing interests.

Received: February 8, 2022
Revised: May 18, 2022
Accepted: July 13, 2022
Published: August 19, 2022

REFERENCES

Baccarini, M., Blasi, E., Puccetti, P., and Bistoni, F. (1983). Phagocytic killing of Candida albicans by different murine effector cells. Med. Mycol. *21*, 271–286. https://doi.org/10.1080/00362178385380431.

Banderas, A., Koltai, M., Anders, A., and Sourjik, V. (2016). Sensory input attenuation allows predictive sexual response in yeast. Nat. Commun. *7*, 12590. https://doi.org/10.1038/ncomms12590.

Bender, A., and Sprague, G.F. (1989). Pheromones and pheromone receptors are the primary determinants of mating specificity in the yeast Saccharomyces cerevisiae. Genetics *121*, 463–476. https://doi.org/10.1093/genetics/121.3.463.

Chou, C.-C., Patel, M.T., and Gartenberg, M.R. (2015). A series of conditional shuttle vectors for targeted genomic integration in budding yeast. FEMS Yeast Res. *15*, 1–9. https://doi.org/10.1093/femsyr/fov010.

Comai, L. (2005). The advantages and disadvantages of being polyploid. Nat. Rev. Genet. *6*, 836–846. https://doi.org/10.1038/nrg1711.

Davis, N., Horecka, J., and Sprague, G. (1993). Cis- and trans-acting functions required for endocytosis of the yeast pheromone receptors. J. Cell Biol. *122*, 53–65. https://doi.org/10.1083/jcb.122.1.53.

de Clare, M., Pir, P., and Oliver, S.G. (2011). Haploinsufficiency and the sex chromosomes from yeasts to humans. BMC Biol. *9*, 15. https://doi.org/10.1186/1741-7007-9-15.

Delneri, D., Hoyle, D.C., Gkargkas, K., Cross, E.J.M., Rash, B., Zeef, L., Leong, H.-S., Davey, H.M., Hayes, A., Kell, D.B., et al. (2008). Identification and characterization of high-flux-control genes of yeast through competition analyses in continuous cultures. Nat. Genet. *40*, 113–117. https://doi.org/10.1038/ng.2007.49.

Dujon, B.A., and Louis, E.J. (2017). Genome diversity and evolution in the budding yeasts (Saccharomycotina). Genetics *206*, 717–750. https://doi.org/10.1534/genetics.116.199216.

Galgoczy, D.J., Cassidy-Stone, A., Llinas, M., O'Rourke, S.M., Herskowitz, I., DeRisi, J.L., and Johnson, A.D. (2004). Genomic dissection of the cell-type-specification circuit in Saccharomyces cerevisiae. Proc. Natl. Acad. Sci. USA *101*, 18069–18074. https://doi.org/10.1073/pnas.0407611102.

Galitski, T., Saldanha, A.J., Styles, C.A., Lander, E.S., and Fink, G.R. (1999). Ploidy regulation of gene expression. Science *285*, 251–254. https://doi.org/10.1126/science.285.5425.251.

Goffeau, A., Barrell, B.G., Bussey, H., Davis, R.W., Dujon, B., Feldmann, H., Galibert, F., Hoheisel, J.D., Jacq, C., Johnston, M., et al. (1996). Life with 6000 genes. Science *274*, 546–567. https://doi.org/10.1126/science.274.5287.546.

Goldstein, A.L., and McCusker, J.H. (1999). Three new dominant drug resistance cassettes for gene disruption inSaccharomyces cerevisiae. Yeast *15*, 1541–1553. https://doi.org/10.1002/(SICI)1097-0061(199910)15:14<1541::AID-YEA476>3.0.CO;2-K.

Haber, J.E. (1974). Bisexual mating behavior in a diploid of Saccharomyces cerevisiae : evidence for genetically controlled non-random chromosome loss during vegetative growth. Genetics *78*, 843–858. https://doi.org/10.1093/genetics/78.3.843.

Hagen, D.C., McCaffrey, G., and Sprague, G.F. (1991). Pheromone response elements are

necessary and sufficient for basal and pheromone-induced transcription of the FUS1 gene of Saccharomyces cerevisiae. Mol. Cell Biol. *11*, 2952–2961. https://doi.org/10.1128/MCB.11.6.2952.

Hailey, D.W., Dams, T.N., and Muller, E.G.D. (2002). Fluorescence resonance energy transfer using color variants of green fluorescent protein. Methods Enzymol. *351*, 34–49. https://doi.org/10.1016/S0076-6879(02)51840-1.

Hanson, S.J., and Wolfe, K.H. (2017). An evolutionary perspective on yeast mating-type switching. Genetics *206*, 9–32. https://doi.org/10.1534/genetics.117.202036.

Harari, Y., Ram, Y., Rappoport, N., Hadany, L., and Kupiec, M. (2018). Spontaneous changes in ploidy are common in yeast. Curr. Biol. *28*, 825–835.e4. https://doi.org/10.1016/j.cub.2018.01.062.

Hartwell, L.H. (1980). Mutants of Saccharomyces cerevisiae unresponsive to cell division control by polypeptide mating hormone. J. Cell Biol. *85*, 811–822. https://doi.org/10.1083/jcb.85.3.811.

Herskowitz, I. (1988). Life cycle of the budding yeast Saccharomyces cerevisiae. Microbiol. Rev. *52*, 536–553. https://doi.org/10.1128/MMBR.52.4.536-553.1988.

Herskowitz, I. (1989). A regulatory hierarchy for cell specialization in yeast. Nature *342*, 749–757. https://doi.org/10.1038/342749a0.

Herskowitz, I., and Jensen, R.E. (1991). Putting the HO gene to work: practical uses for mating-type switching. Methods Enzymol. *194*, 132–146. https://doi.org/10.1016/0076-6879(91)94011-z.

Hochstrasser, M., and Varshavsky, A. (1990). In vivo degradation of a transcriptional regulator: the yeast α2 repressor. Cell *61*, 697–708. https://doi.org/10.1016/0092-8674(90)90481-S.

Jenness, D.D., and Spatrick, P. (1986). Down regulation of the α-factor pheromone receptor in S. cerevisiae. Cell *46*, 345–353. https://doi.org/10.1016/0092-8674(86)90655-0.

Johnson, A.D. (1995). Molecular mechanisms of cell-type determination in budding yeast. Curr. Opin. Genet. Dev. *5*, 552–558. https://doi.org/10.1016/0959-437X(95)80022-0.

Johnson, P.R., Swanson, R., Rakhilina, L., and Hochstrasser, M. (1998). Degradation signal masking by heterodimerization of MATα2 and MATa1 blocks their mutual destruction by the ubiquitin-proteasome pathway. Cell *94*, 217–227. https://doi.org/10.1016/S0092-8674(00)81421-X.

Jones, J.S., and Prakash, L. (1990). Yeast Saccharomyces cerevisiae selectable markers in pUC18 polylinkers. Yeast *6*, 363–366. https://doi.org/10.1002/yea.320060502.

Keleher, C.A., Goutte, C., and Johnson, A.D. (1988). The yeast cell-type-specific repressor α2 acts cooperatively with a non-cell-type-specific protein. Cell *53*, 927–936. https://doi.org/10.1016/S0092-8674(88)90449-7.

Kellis, M., Birren, B.W., and Lander, E.S. (2004). Proof and evolutionary analysis of ancient genome duplication in the yeast Saccharomyces cerevisiae. Nature *428*, 617–624. https://doi.org/10.1038/nature02424.

Khmelinskii, A., Meurer, M., Duishoev, N., Delhomme, N., and Knop, M. (2011). Seamless gene tagging by endonuclease-driven homologous recombination. PLoS One *6*, e23794. https://doi.org/10.1371/journal.pone.0023794.

Klar, A.J.S. (1987). Determination of the yeast cell lineage. Cell *49*, 433–435. https://doi.org/10.1016/0092-8674(87)90442-9.

Kumaran, R., Yang, S.-Y., and Leu, J.-Y. (2013). Characterization of chromosome stability in diploid, polyploid and hybrid yeast cells. PLoS One *8*, e68094. https://doi.org/10.1371/journal.pone.0068094.

Laney, J.D., and Hochstrasser, M. (2003). Ubiquitin-dependent degradation of the yeast Matα2 repressor enables a switch in developmental state. Genes Dev. *17*, 2259–2270. https://doi.org/10.1101/gad.1115703.

Lim, F.-L., Hayes, A., West, A.G., Pic-Taylor, A., Darieva, Z., Morgan, B.A., Oliver, S.G., and Sharrocks, A.D. (2003). Mcm1p-Induced DNA bending regulates the formation of ternary transcription factor complexes. Mol. Cell Biol. *23*, 450–461. https://doi.org/10.1128/MCB.23.2.450-461.2003.

Longtine, M.S., Mckenzie, A., III, Demarini, D.J., Shah, N.G., Wach, A., Brachat, A., Philippsen, P., and Pringle, J.R. (1998). Additional modules for versatile and economical PCR-based gene deletion and modification in Saccharomyces cerevisiae. Yeast *14*, 953–961. https://doi.org/10.1002/(SICI)1097-0061(199807)14:10<953::AID-YEA293>3.0.CO;2-U.

Marcet-Houben, M., and Gabaldón, T. (2015). Beyond the whole-genome duplication: phylogenetic evidence for an ancient interspecies hybridization in the baker's yeast lineage. PLoS Biol. *13*, e1002220. https://doi.org/10.1371/journal.pbio.1002220.

Maruyama, Y., Ito, T., Kodama, H., and Matsuura, A. (2016). Availability of amino acids extends chronological lifespan by suppressing hyper-acidification of the environment in Saccharomyces cerevisiae. PLoS One *11*, e0151894. https://doi.org/10.1371/journal.pone.0151894.

Mateus, C., and Avery, S.V. (2000). Destabilized green fluorescent protein for monitoring dynamic changes in yeast gene expression with flow cytometry. Yeast *16*, 1313–1323. https://doi.org/10.1002/1097-0061(200010)16:14<1313::AID-YEA626>3.0.CO;2-O.

Matsui, A., Kamada, Y., and Matsuura, A. (2013). The role of autophagy in genome stability through suppression of abnormal mitosis under starvation. PLoS Genet. *9*, e1003245. https://doi.org/10.1371/journal.pgen.1003245.

Mayer, V.W., and Aguilera, A. (1990). High levels of chromosome instability in polyploids of Saccharomyces cerevisiae. Mutat. Res. *231*, 177–186. https://doi.org/10.1016/0027-5107(90)90024-X.

Morard, M., Benavent-Gil, Y., Ortiz-Tovar, G., Pérez-Través, L., Querol, A., Toft, C., and Barrio, E. (2020). Genome structure reveals the diversity of mating mechanisms in Saccharomyces cerevisiae x Saccharomyces kudriavzevii hybrids, and the genomic instability that promotes phenotypic diversity. Microb. Genom. *6*. https://doi.org/10.1099/mgen.0.000333.

Morrill, S.A., and Amon, A. (2019). Why haploinsufficiency persists. Proc. Natl. Acad. Sci. USA *116*, 201900437. https://doi.org/10.1073/pnas.1900437116.

Natarajan, A., Subramanian, S., and Srienc, F. (1998). Comparison of mutant forms of the green fluorescent protein as expression markers in Chinese hamster ovary (CHO) and Saccharomyces cerevisiae cells. J. Biotechnol. *62*, 29–45. https://doi.org/10.1016/S0168-1656(98)00040-6.

Nixon, C.E., Wilcox, A.J., and Laney, J.D. (2010). Degradation of the Saccharomyces cerevisiae mating-type regulator α1: genetic dissection of Cis -determinants and trans -acting pathways. Genetics *185*, 497–511. https://doi.org/10.1534/genetics.110.115907.

Otto, S.P. (2007). The evolutionary consequences of polyploidy. Cell *131*, 452–462. https://doi.org/10.1016/j.cell.2007.10.022.

Paliwal, S., Iglesias, P.A., Campbell, K., Hilioti, Z., Groisman, A., and Levchenko, A. (2007). MAPK-mediated bimodal gene expression and adaptive gradient sensing in yeast. Nature *446*, 46–51. https://doi.org/10.1038/nature05561.

Payseur, B.A., Presgraves, D.C., and Filatov, D.A. (2018). Introduction: sex chromosomes and speciation. Mol. Ecol. *27*, 3745–3748. https://doi.org/10.1111/mec.14828.

Rivers, D.M., and Sprague, G.F. (2003). Autocrine activation of the pheromone response pathway in matα2 - cells is attenuated by SST2- and ASG7-dependent mechanisms. Mol. Genet. Genom. *270*, 225–233. https://doi.org/10.1007/s00438-003-0914-3.

Roberts, C.J., Nelson, B., Marton, M.J., Stoughton, R., Meyer, M.R., Bennett, H.A., He, Y.D., Dai, H., Walker, W.L., Hughes, T.R., et al. (2000). Signaling and circuitry of multiple MAPK pathways revealed by a matrix of global gene expression profiles. Science *287*, 873–880. https://doi.org/10.1126/science.287.5454.873.

Roth, A.F., Nelson, B., Boone, C., and Davis, N.G. (2000). Asg7p-Ste3p inhibition of pheromone signaling: regulation of the zygotic transition to vegetative growth. Mol. Cell Biol. *20*, 8815–8825. https://doi.org/10.1128/mcb.20.23.8815-8825.2000.

Shin, D.Y., Yun, J.H., and Yoo, H.S. (1997). Novel strategy for isolating suppressors of meiosis-deficient mutants and its application for isolating the bcy1 suppressor. J. Microbiol. 61–65.

Siekhaus, D.E., and Drubin, D.G. (2003). Spontaneous receptor-independent heterotrimeric G-protein signalling in an RGS mutant. Nat. Cell Biol. *5*, 231–235. https://doi.org/10.1038/ncb941.

Sikorski, R.S., and Boeke, J.D. (1991). [20] in vitro mutagenesis and plasmid shuffling: from cloned gene to mutant yeast. Methods Enzymol. 302–318. https://doi.org/10.1016/0076-6879(91)94023-6.

Sorrells, T.R., Booth, L.N., Tuch, B.B., and Johnson, A.D. (2015). Intersecting transcription networks constrain gene regulatory evolution. Nature *523*, 361–365. https://doi.org/10.1038/nature14613.

Strathern, J., Hicks, J., and Herskowitz, I. (1981). Control of cell type in yeast by the mating type locus. J. Mol. Biol. *147*, 357–372. https://doi.org/10.1016/0022-2836(81)90488-5.

Strazdis, J.R., and MacKay, V.L. (1983). Induction of yeast mating pheromone a-factor by α cells. Nature *305*, 543–545. https://doi.org/10.1038/305543a0.

Takahashi, S., and Pryciak, P.M. (2008). Membrane localization of scaffold proteins promotes graded signaling in the yeast MAP kinase cascade. Curr. Biol. *18*, 1184–1191. https://doi.org/10.1016/j.cub.2008.07.050.

Tanaka, H., and Yi, T.-M. (2009). Synthetic morphology using alternative inputs. PLoS One *4*, e6946. https://doi.org/10.1371/journal.pone.0006946.

Tsong, A.E., Miller, M.G., Raisner, R.M., and Johnson, A.D. (2003). Evolution of a combinatorial transcriptional circuit. Cell *115*, 389–399. https://doi.org/10.1016/S0092-8674(03)00885-7.

Tsong, A.E., Tuch, B.B., Li, H., and Johnson, A.D. (2006). Evolution of alternative transcriptional circuits with identical logic. Nature *443*, 415–420. https://doi.org/10.1038/nature05099.

Udden, M.M., and Finkelstein, D.B. (1978). Reaction order of Saccharomyces cerevisiae alpha-factor-mediated cell cycle arrest and mating inhibition. J. Bacteriol. *133*, 1501–1507. https://doi.org/10.1128/jb.133.3.1501-1507.1978.

Wach, A., Brachat, A., Pöhlmann, R., and Philippsen, P. (1994). New heterologous modules for classical or PCR-based gene disruptions inSaccharomyces cerevisiae. Yeast *10*, 1793–1808. https://doi.org/10.1002/yea.320101310.

Wach, A., Brachat, A., Alberti-Segui, C., Rebischung, C., and Philippsen, P. (1997). HeterologousHIS3 marker and GFP reporter modules for PCR-targeting inSaccharomyces cerevisiae. Yeast *13*, 1065–1075. https://doi.org/10.1002/(SICI)1097-0061(19970915)13:11<1065::AID-YEA159>3.0.CO;2-K.

Wolfe, K.H., and Shields, D.C. (1997). Molecular evidence for an ancient duplication of the entire yeast genome. Nature *387*, 708–713. https://doi.org/10.1038/42711.

Zhang, N.-N., Dudgeon, D.D., Paliwal, S., Levchenko, A., Grote, E., and Cunningham, K.W. (2006). Multiple signaling pathways regulate yeast cell death during the response to mating pheromones. Mol. Biol. Cell *17*, 3409–3422. https://doi.org/10.1091/mbc.e06-03-0177.

STAR★METHODS

KEY RESOURCES TABLE

REAGENT or RESOURCE	SOURCE	IDENTIFIER
Antibodies		
Mouse monoclonal anti-Myc	MBL	Cat#M047-3; RRID: AB_592470
Mouse monoclonal anti-GFP	Wako	Cat#012-22541; RRID: AB_2922809
Anti-mouse IgG, HRP-linked Antibody	Cell Signaling technology	Cat#7076; RRID: AB_330924
Chemicals, peptides, and recombinant proteins		
5-fluoroorotic acid	Apollo Scientific	Cat#PC4054
G418 Disulfate	nacalai tesque	Cat#16512-94
Hygromycin B	nacalai tesque	Cat#07296-24
Nourseothricin	JENABIO	Cat#AB-102L
Propidium iodite	Wako	Cat#164-16721
ImmunoStar Zeta	Wako	Cat#297-72403
RNase A	nacalai tesque	Cat#30142-04
proteinase K	nacalai tesque	Cat#29442-85
Deposited data		
Raw data of images	This paper	Mendeley data: https://doi.org/10.17632/kfg8k65w7w.2
Experimental models: Organisms/strains		
All *Saccharomyces cerevisiae* strains used in this study are of the BY4742 strain background and are listed in Table S1	Matsuura Lab	N/A
Oligonucleotides		
See Table S2 for a list of oligonucleotides.	This study	N/A
Recombinant DNA		
See Table S3 for a list of Recombinant DNA.	See Table S3	N/A
Software and algorithms		
BZ-X800 Viewer	Keyence	N/A
Deltavision softWoRx	Applied Precision	N/A
CytExpert software	Beckman Coulter	N/A
R	R	N/A
ImageJ	ImageJ	N/A
Fiji	Fiji team	N/A

RESOURCE AVAILABILITY

Lead contact

Further information and requests for resources and reagents should be directed to and will be fulfilled by the lead contact, Akira Matsuura (amatsuur@faculty.chiba-u.jp).

Materials availability

Strains generated in this study will be deposited to National BioResource Project-Yeast.

Data and code availability

- Original western blot images have been deposited at Mendeley and are publicly available as of the date of publication. The DOI is listed in the key resources table. Microscopy data reported in this paper will be shared by the lead contact upon request.

- This paper does not report original code.
- Any additional information required to reanalyze the data reported in this paper is available from the lead contact upon request.

EXPERIMENTAL MODEL AND SUBJECT DETAILS

The yeast strains used in this study are listed in Table S1. All strains were derived from BY4742. Gene disruption and tagging were conducted using the conventional one-step PCR-mediated method (Longtine et al., 1998). Polyploid strains were created by mating, and their ploidy was confirmed by DNA content measurement as described below. Yeast cells were grown in YPD medium, consisting of 1% yeast extract (BD Biosciences, San Jose, CA), 2% hipolypepton (Nihon Pharmaceutical Corporation, Tokyo, Japan), and 2% glucose (Nacalai Tesque, Kyoto, Japan), SD consisting of 0.17% yeast nitrogen base without amino acids and ammonium sulfate (BD Biosciences), 0.5% $(NH_4)_2SO_4$ (Wako Pure Chemical Industries, Ltd., Osaka, Japan), and 2% glucose, SC supplementing amino acids and nucleobases to SD medium at the concentrations described previously (Maruyama et al., 2016), and SDCA supplementing 0.5% casamino acid (BD Biosciences) to SD medium. KanMX, hphMX and natMX strain selections were performed in YPD plates containing 250 μg/mL G418, 300 μg/mL Hygromycin B and 100 μg/mL Nourseothricin, respectively. Yeast strains used in the presented experiments are as follows:

Figure 1

(A) OYA1320, OYA1321, OYA1322, OYA228, OYA1343, OYA1344, OYA1332, OYA1334; (B) OYA1320, OYA1321, OYA1322, OYA228, OYA1343, OYA1344, OYA1332, OYA1334, OYA1351, OYA1352, OYA1353, OYA1398, OYA569; (C) BY4742, OYA1, OYA1320, OYA28, OYA1343, OYA1351, OYA1321, OYA356, OYA1344, OYA1352, OYA1322, OYA228, OYA1332, OYA1353, OYA1398, OYA569; (D) OYA1351, OYA1352, OYA1353; (E) OYA1398, OYA569.

Figure 2

(A, B) OYA449, OYA798, OYA799, OYA800.

Figure 3

(A) OYA1320, OYA1321, OYA1322, YOM22, OYA254, OYA255, OYA412, OYA126, OYA369, OYA370, OYA415, OYA280, OYA377, OYA378, OYA418, OYA281, OYA349, OYA350, OYA421; (B) YOM22, OYA126, OYA280, OYA281, OYA254, OYA369, OYA377, OYA349, OYA255, OYA370, OYA378, OYA350, OYA412, OYA415, OYA418, OYA421.

Figure 4.

(A) OYA121, OYA115, OYA809, OYA1395, OYA103, OYA777; (B) OYA121, OYA115, OYA103, OYA777; (C) OYA868, OYA1192, OYA961, OYA962, OYA963, OYA1242, OYA1250.

Figure 5

(A) OYA503, YOM22, OYA1039, OYA254, OYA255, OYA412, OYA233, YOM37; (B) OYA1366, OYA1367, OYA1368.

Figure S1

OYA800, OYA228.

Figure S2

BY4742, OYA1, OYA1322, OYA1332.

Figure S3

OYA1343, OYA1366, OYA1344, OYA1367, OYA1332, OYA1368.

Figure S4

OYA381, OYA1407, OYA1408, OYA1409, OYA1410.

METHOD DETAILS

Yeast strains, plasmids, and media

To construct a completely isogenic strain, the mating type of BY4742 was artificially converted from α to a to create OYA38 (BY4742 *MAT*a). First, BY4742 was transformed with YCp50-GAL-HO (Herskowitz and Jensen, 1991), then *HO* was induced by culturing in medium containing galactose (0.17% yeast nitrogen base without amino acids or ammonium sulfate, 0.5% $(NH_4)_2SO_4$, 0.5% casamino acid and 3% galactose (Nacalai Tesque, Kyoto, Japan)) at 30°C for 6 h. Second, the culture was spread on a SDCA plate and formed a single colony. Third, those responsive to α-factor were selected, and then those losing the plasmid were selected in a medium containing 5-fluoroorotic acid.

OYA1 (BY4742 *mat*::*kanMX*) was created by transformation of *mat*Δ with a PCR-based *mat*::*kanMX* deletion cassette generated by amplifying *kanMX* from pFA6a-kanMX (Wach et al., 1994) using primers, MAT del F and MAT del R. Transformants were confirmed by PCR using primers, MAT check F and MAT check R, and sensitivity to α-factor.

*MAT*α/*MAT*α diploid strains were created by rare-mating. To construct a *MAT*α/*MAT*α diploid strain, *MAT*α haploid strains were transformed with plasmids with different auxotrophic markers (pRS313, pRS315) (Baccarini et al., 1983), mixed and cultured overnight on YPD medium plate, and then selected on a SC -Leu -His medium plate in which only the zygote could grow. Then, plasmids were naturally lost by incubation in YPD medium. In the same way, *MAT*α/*MAT*α/*MAT*α triploid strains were constructed by mating a *MAT*α haploid strain and a *MAT*α/*MAT*α diploid strain, and *MAT*α/*MAT*α/*MAT*α/*MAT*α tetraploid strains were constructed by mating *MAT*α/*MAT*α diploid strains with each other. These strains were confirmed to be α-mating type by assessing the formation of sexual agglutination in a co-culture with the *MAT*a tester but not with the *MAT*α tester.

*mat*Δ/*mat*Δ diploid strains were created by mating by complementation of *mat*Δ with *MAT*a-harbored YCpMATa or *MAT*α-harbored YCpMATα plasmid, restoring fertility as an intact a- or α-mating type, respectively. To construct a *mat*Δ/*mat*Δ diploid strain, *mat*Δ strains were transformed with YCpMATa or YCpMATα (Shin et al., 1997) and plasmids with different auxotrophic markers (pRS313, pRS315), mixed and cultured overnight on YPD medium plate, selected on a SC -Leu –His -Ura medium plate in which only the zygote could grow, and then selected for loss of YCpMATa and YCpMATα on 5-FOA medium (0.17% yeast nitrogen base without amino acids and ammonium sulfate, 0.5% $(NH_4)_2SO_4$, 0.5% casamino acid, 0.1% 5-fluoroorotic acid, 50 μg/mL uracil and 2% gulcose) plate. Then, cells that lost auxotrophic marker plasmids by incubation in YPD medium were picked up. Similarly, *mat*Δ/*mat*Δ/*mat*Δ triploid strains were created by mating a *mat*Δ haploid strain and a *mat*Δ/*mat*Δ diploid strain, and a *mat*Δ/*mat*Δ/*mat*Δ/*mat*Δ tetraploid strain were created by mating *mat*Δ/*mat*Δ diploid strains with each other. These strains were confirmed to be a-mating type by assessing the formation of sexual agglutination in a co-culture with the *MAT*α tester but not with the *MAT*a tester.

*mat*Δ/*MAT*α diploid strains (M/G ratio mutants) were created by mating. To construct a *mat*Δ/*MAT*α diploid strain, a *mat*Δ strain with YCpMATa and a *MAT*α haploid strain with pRS313 mixed and cultured overnight on YPD medium plate and selected on a SC -His -Ura medium plate in which only the zygote could grow. Then selected for loss of YCpMATa on 5-FOA medium plate. Then, cells that lost pRS313 by incubation in YPD medium were picked up. Similarly, *mat*Δ/*mat*Δ/*MAT*α triploid strains were created by mating a *mat*Δ/*mat*Δ diploid strain and a *MAT*α haploid strain, and *mat*Δ/*mat*Δ/*mat*Δ/*MAT*α tetraploid strains were created by mating a *mat*Δ/*mat*Δ/*mat*Δ triploid strain and a *MAT*α haploid strain. These strains were confirmed by PCR using primers, MAT check F and MAT check R, to have two distinct products corresponding to *MAT*α and *mat*Δ.

Similarly, the M/G ratio mutant strains shown in Figure 3 were created by mating. First, strains with M/G ratio = 2 (OYA126 *MATα ho*::*MATα*), = 3 (OYA280 *MATα ho*::*MATα* Chr3::*MATα*) and = 4 (OYA281 *MATα ho*::*MATα* Chr3::*MATα* Chr14::*MATα*) were created by sequential introduction of ectopic *MATα* constructs. Then, the M/G ratio mutant strains were constructed by mating strains having ectopic *MATα* with each ploidy strain of *mat*Δ.

In the mating of M/G ratio mutant strains and *MAT*a strain, the strains were also each transformed with plasmids with different auxotrophic markers (pRS313, pRS315), mixed and cultured overnight on YPD medium plate, selected on a SC -Leu -His medium plate in which only the zygote could grow. Then, auxotrophic marker plasmids were naturally lost by incubation in YPD medium.

Since *ste4*Δ strains were not capable of mating, pRS317-*STE4* was transformed to restore fertility, and *ste4*Δ M/G ratio mutants were produced using the method for producing M/G ratio mutants described above.

The mating type reporters are two constructs expressing *MFA1* promoter-driven *GFP* and *MFALPHA1* promoter-driven *mCherry* introduced into intergenic region between *SAM50* and *SSN8* on Chromosome XIV and *HO* locus on Chromosome IV, respectively.

To construct cells harboring Chr14::*MFA1pr-GFP-kanMX*, two PCR fragments were isolated, one amplified with the primers M13U-MFA1P F and NLS-MFA1P R using genomic DNA of BY4742 strain as a template, and the other amplified with the primers NLS-F1 F and Chr14 R using the plasmid pFA6a-GFP(S65T)-kanMX6 (Wach et al., 1997) as a template, resulting the two PCR products were *MFA1* promoter and *GFP-kanMX* sequence. Then, the two resulting fragments were amplified using overlapping PCR with the primers Chr14-M13U F and Chr14 R. The final PCR product was transformed into Chromosome XIV (Location: Chromosome XIV 583,958^583,959) and correct insertion was confirmed by PCR.

Cells harboring *ho*::*MFALPHA1pr-mCherry-hphMX* was constructed in the same way using the corresponding primers (M13U-MFALPHA1P F, NLS-MFALPHA1P R, HO-R1 R and HO-M13U F), and the plasmid pBS35 (Hailey et al., 2002) as a template.

The *FUS1pr*-GFP reporter is a construct expressing *FUS1* promoter-driven *GFP* into *HO* locus. To construct cells harboring *ho*::*FUS1pr-GFP-kanMX*, a *fus1*::*FUS1pr*-GFP strain was first constructed through the conventional one-step PCR-based gene replacement. The *fus1*::*FUS1pr-GFP* strain was created by replacing the *FUS1* ORF of BY4742 with PCR product containing the *GFP* gene and the *kanMX* marker gene, using amplified with the primers FUS1pr-F1 F and FUS1 del R and the plasmid pFA6a-GFP(S65T)-kanMX6 as a template. Transformants expressing the GFP from the *FUS1* promoter were selected on plates containing G418. Next, to construct a strain in which the *HO* gene was replaced with *FUS1pr*-GFP, a fragment was amplified with the primers M13U-FUS1pr F and HO-R1 R using genomic DNA of the *fus1*::*FUS1pr*-GFP strain as a template, and then using that fragment as a template, *ho*::*FUS1pr-GFP-kanMX* fragment was amplified with the primers HO-M13U F and HO-R1 R. Transformants were selected on plates containing G418 and correct insertion of the fragment was confirmed by PCR.

To quantify Matα1 and Matα2 by Western blotting, Myc and GFP were tagged, respectively. Strains expressing Matα1-13Myc were generated by the conventional one-step PCR-based transformation, using the primers MATα1 Ctag F, MATα1 Ctag R, and the plasmid pFA6a-13Myc-kanMX6 (Longtine et al., 1998). Transformants expressing *MATα1-13Myc* were selected on plates containing G418. Strains expressing GFP-Matα2 were generated by PCR-based transformation and subsequent marker excision described previously (Khmelinskii et al., 2011), using the primers MATα2 Ntag F and MATα2 Ntag R, and the plasmid pMaM189. First, cells in which the amplified fragment was introduced to express GFP-Matα2 from the *NOP1* promoter were selected on SDCA plates. Then, cells which express *GFP-MATα2* from the *MATα2* promoter were selected in a medium containing 5-fluoroorotic acid. Those selected were cells in which the *URA3-NOP1* promoter sequence was popped out by homologous recombination. Correct insertion of the fragment was confirmed by PCR.

Ectopic *MATα* is defined as *MATα* (*MATα1* and *MATα2*) genes introduced at different locus from the native *MAT* locus. In this study, constructs *ho*::*MATα*, Chr3::*MATα*, and Chr14::*MATα* were generated to introduce *MATα*

genes at three different locus, *HO* on Chromosome IV, intergenic region between *YCRWdelta11* and *FEN2* on Chromosome III, and intergenic region between *SAM50* and *SSN8* on Chromosome XIV, respectively. To construct ectopic *MATα* strains, three strains, each with a selection marker gene near *MAT* locus, were constructed through PCR-based gene insertion. The downstream region of *MATα* was replaced with PCR products containing the selection marker gene and homologous flanking regions downstream of *MATα*.

To construct the *ho*::*MATα-His3MX* strain, the PCR products were amplified with the primers MATα down marker F and MATα down marker R using the plasmid pFA6a-His3MX6 (Wach et al., 1997) as a template. The strain transformed with this PCR product is the *MATα-His3MX* strain, which has *His3MX* downstream of their *MAT* locus. Next, the fragment was amplified using genomic DNA of the *MATα-His3MX* strain as a template with the primers M13U-MATα up F and MATα check R. Then, using that resulting fragment as a template, *ho*::*MATα-His3MX* construct was further amplified using the primers HO-M13U F and HO-R1 R, resulting to replace *HO* gene with *MATα-His3MX*.

Chr 3::*MATα-kanMX* strain and Chr 14::*MATα-natMX* strain were constructed in the same way using the corresponding primers (Chr3-M13U F, Chr3R, Chr14-M13U F, Chr14R) and plasmids (pFA6a-kanMX6 and pFA6a-natMX6 (Goldstein and McCusker, 1999)). The final PCR products were transformed into Chromosome III (Location: Chromosome III 170,287^170,288) and Chromosome XIV (Location: Chromosome XIV 583,958^583,959), and correct insertion was confirmed by PCR.

To construct *MATα1* overexpression strains, native *MATα1* promoter was replaced with a PCR product containing homologous flanking regions upstream of *MATα1* ORF and *TEF1* promoter or *NOP1* promoter. The PCR products were amplified with the primers MATα1 Ntag F and MATα1 Ntag R, and the plasmid pMaM173 or pMaM189 (Khmelinskii et al., 2011) as a template. Correct insertion of the fragment was confirmed by PCR.

MATα2 overexpression strains were constructed in the same way using the corresponding primers (MATα2 Ntag F and MATα2 Ntag R).

Auxotrophic mutations were rescued by sequential integration of the corresponding wild-type genes as described previously (Maruyama et al., 2016). *ura3* and *lys2* mutations were complemented by PCR fragments amplified from genomic DNA; *URA3* fragments was amplified with the primers URA3 up and URA3 down using genomic DNA of X2180-1A, and *LYS2* fragments was amplified with the primers LYS2 up and LYS2 down using genomic DNA of BY4741. *his3* and *leu2* mutations were complemented by fragments cloned on plasmids; *HIS3* fragment was cut out by *Bam*HI and *Xho*I from pJJ215 (Jones and Prakash, 1990), and *LEU2* fragment was cut out by *Hpa*I and *Sal*I from pJJ283 (pJJ252) (Jones and Prakash, 1990). Transformants were then selected by SDCA, SC –Lys, SC –His, or SC –Leu plates.

To construct the plasmid pRS317-*STE4*, the *STE4* fragment was amplified with the primers STE4 GRC F and STE4 GRC R using genomic DNA of BY4742 strain as a template. The fragment was cotransformed into the *ste4Δ* strain with *Hin*dIII and *Sac*I–digested pRS317 (Sikorski and Boeke, 1991), and the gap-repaired plasmid was then isolated from the transformant.

Microscopy

Yeast cells grown to late log phase in overnight culture were collected by centrifugation (3,000 rpm for 30 s), and then the cells were observed. Fluorescence microscopy was performed by DeltaVision (Applied Precision, Issaquah, WA) and Bright field microscopy was performed by BZ-X810 (Keyence, Osaka, Japan). Images taken in DeltaVision were captured using softWoRx image acquisition and analysis software.

For quantification of cell morphology, overnight culture was stained with FITC-ConA for 30 min, washed with PBS, imaged with BZ-X810, and analyzed with ImageJ.

Analysis of mating type reporters

Yeast cells were grown to log phase and resuspended in PBS. Flow cytometric analysis was conducted with the CytoFLEX S flow cytometer with 488-nm (for GFP) and 561–nm (for mCherry) lasers (Beckman Coulter, Brea, CA). Approximately 10,000 events were acquired for each sample.

Analysis of *FUS1pr*-GFP reporter

Yeast cells were grown to log phase and resuspended in PBS containing 1 μg/mL Propidium iodide (PI). Flow cytometric analysis was conducted with the CytoFLEX S flow cytometer with 488-nm (for GFP) and 561–nm (for PI) lasers. Dead cells detected by PI staining were excluded, and approximately 10,000 events were acquired for each sample.

Quantification of live/dead cells

Yeast cells were grown to log phase and resuspended in PBS containing 1 μg/mL PI at room temperature for 10 min. Microscopic analysis was conducted with the BZ-X810. At least 200 cells were scored for every strain and the percentage of dead cells stained with PI was calculated.

Mating test

A single colony of each sample strain was picked up with a sterile toothpick and spread as a separate thick vertical strip. On a separate YPD plate, tester strains were spread in the same way. The two plates were incubated at 30°C overnight. By replica plating, strips from the plate of the sample strain were stamped onto a new YPD plate through a sterile velvet cloth. Then, tester strains were transferred to another velvet cloth in the same way, and stamped so that tester strains and sample strains were oriented perpendicular to each other onto the YPD plate that already had sample strains. The plate was incubated overnight at 30°C, then stamped through a sterile velvet cloth into a selective medium in which only zygotes could grow, and incubated at 30°C for 3 days.

Western blot analysis

Protein extraction was performed based on alkaline-trichloroacetic acid method with some modifications. 1.0 OD600 unit of cells was removed from culture, pelleted and stored at −80°C. The pellets were suspended in 200 μL of an alkaline solution (1.85 M NaOH-7.4% 2-mercaptoethanol) and incubated on ice for 10 min. Then, 200 μL of 50% trichloroacetic acid was added and incubated on ice for 10 min. Samples were boiled for 5 min prior to SDS/polyacrylamide gel electrophoresis (SDS/PAGE) and transferred to polyvinylidene difluoride membrane (Millipore, Billerica, MA, USA). Immunoblot analysis was performed with the indicated antibodies, and the immunoreactive proteins were visualized using ImmunoStar Zeta (Wako Pure Chemical Industries, Ltd.).

DNA content measurement

Flow cytometry analysis method were modified from a previous study (Matsui et al., 2013). Cells were grown overnight and fixed with 70% ethanol at 4°C overnight. Then the cells were washed and suspended in 50 mM sodium citrate, treated with 250 μg/mL RNase A at 50°C for 1 h, and then treated with 1 mg/mL proteinase K at 50°C for 1 h. The resuspended cells were stained with 16 μg/mL propidium iodide at room temperature for 30 min. The DNA content of cells was measured on a CytoFLEX S flow cytometer.

Spot assay

Yeast cells grown to log phase were counted on a haemocytometer and diluted with DW to 1 × 10^7 cells/ml. The diluted solutions were serially diluted 10-fold and then spotted onto SDCA plate medium. Colonies were photographed after 2 days.

QUANTIFICATION AND STATISTICAL ANALYSIS

Statistical analysis were performed using statistical software R (Figures 1B, 1C, 3B, 4C, and S3).

Microscopy image analysis

For analysis of cell size, roundness, and slenderness, images of cells stained with FITC-ConA were analyzed with ImageJ. Each parameter calculated as Area, Circularity, and Major axis/Minor axis (Fit Ellipse) in Analyze Particles, respectively. For each strain, 30 unbudded cells were measured.